# Quantitative Characterization of the Flexibility of Poly(ethylene glycol) Chains Attached to a Glassy Carbon Electrode

**Agnès Anne* and Jacques Moiroux**

*Laboratoire d'Electrochimie Moléculaire, Unité Mixte de Recherche Université—CNRS No. 7591, Université de Paris 7—Denis Diderot, 2 place Jussieu, 75251 Paris, Cedex 05, France*

*Received April 12, 1999; Revised Manuscript Received June 15, 1999*

ABSTRACT: Electrodes bearing terminally attached $PEG_{600}$−Fc and $PEG_{3400}$−Fc chains exhibit remarkably similar time responses in cyclic voltammetry. Two asymmetrical NHS−$PEG_{600}$−Fc and NHS−$PEG_{3400}$−Fc poly(ethylene glycol) (PEG) chains of markedly different lengths were synthesized, and their activated *N*-hydroxysuccinimide ester (NHS) end was used for terminal attachment to the surface of a glassy carbon electrode. A similar surface coverage was obtained with both derivatives. At this coverage, the attached NHS−$PEG_{600}$−Fc, which are relatively small, were not constrained to overlap whereas the attached NHS−$PEG_{3400}$−Fc were necessarily stretched. The presence of the ferrocene (Fc) redox probe gave rise to signals in cyclic voltammetry which were analyzed quantitatively. At sufficiently high potential scan rate the peak currents reflect the flexibility of the terminally attached PEG chains. Both types of derivatized electrodes gave remarkably similar peak currents in cyclic voltammetry.

## Introduction

Chemical modification of electrode surfaces has become quite common.[1] Our aim is the attachment of poly(ethylene glycol) (PEG) chains in such a manner that one end of each PEG chain is covalently bound to the electrode surface and the other end bears a redox probe, as sketched in Chart 1.

PEG molecules bearing an *N*-hydroxysuccinimide (NHS) activated ester at one end and the ferrocenyl (Fc) redox probe at the other end were synthesized for the first time, the average PEG molar weights being either 600 (NHS−$PEG_{600}$−Fc) or 3400 (NHS−$PEG_{3400}$−Fc). The covalent binding to the electrode was achieved by reaction of a NHS−$PEG_{MW}$−Fc solution with amino groups generated on the glassy carbon surface when the disk electrode was polished in the presence of ammonia as reported for the covalent attachment of other NHS esters to the same electrode material.[2,3] In the present work the reaction between NHS−$PEG_{MW}$−Fc and the electrode surface was even achieved in aqueous media with quite low amounts of the NHS−$PEG_{MW}$−Fc reagent.

The chemical modification of the glassy carbon electrode by attachment of PEG polymers investigated here is different from that in which polymer formation is initiated and developed at electrode surfaces[1] or from compact self-assembled monolayers on a gold electrode.[4]

The PEG backbone was chosen for several reasons. The average chain length of this polydispersed polymer can be varied almost at will, since the range of average molar weights (MW) of commercially available PEG's is large. The PEG polymers are soluble in polar organic solvents as well as in water, and their tendency to self-assemble is much weaker than that of lipids. Due to the intrinsic heterogeneity of the glassy carbon surface, the monolayer of attached PEG molecules cannot be tightly compact. Under such conditions the Fc redox probe needs to reach the electrode surface to transfer an electron. Thus, the chain flexibility may kinetically control the resulting current. The excitation and measurement technique used in the present is cyclic voltammetry. At high potential scan rates, the cyclic voltammograms provide evidence of kinetic control by the PEG chain flexibility, which can be characterized quantitatively.

**Chart 1**

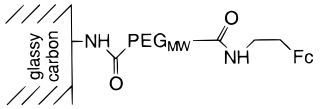


## Experimental Section

**Materials**. Poly(ethylene glycol) (PEG) 600 diacid, *O*,*O*′-bis(2-carboxymethyl)poly(ethylene glycol) 600 ($PEG_{600}$−$(CO_2H)_2$), and poly(ethylene glycol) 2000 diacid were purchased from Fluka and analyzed by TLC and $^1$H NMR techniques. It was then established that the poly(ethylene glycol) 2000 diacid product had a formula and an average molecular weight in disagreement with the manufacturer's specifications. Therefore, we did not synthesize a NHS−$PEG_{2000}$−Fc derivative. Poly(ethylene glycol) 3400 monoacid, *O*-(2-carboxyethyl)poly(ethylene glycol) 3400 (OH−$PEG_{3400}$−$CO_2H$), *O*-2-[*N*-hydroxysuccinimidyl)ethyloxy carbonyl], and *O*′-2-(*N*-biotinamidoethyl)poly(ethylene glycol) 3400 (NHS−$PEG_{3400}$−Biotin) were from Shearwater Polymers (Huntsville, AL). *β*-Aminoethylferrocene was prepared as previously described.[3] It decomposed when stored and was freshly purified by column chromatography before each use (silica gel, 15% methanol in chloroform). Anhydrous analytical grade dichloromethane was used as received from SDS. The supporting electrolyte tetrabutylammonium hexafluorophosphate ($NBu_4PF_6$) (99+%) was purchased from Fluka. Thin-layer chromatographic (TLC) analyses were performed on 0.25 mm silica gel Polygram SIL G/$UV_{254}$ plates. Iodine vapor was used as a reagent for visualization of PEGs. Preparative column chromatography was carried over Magerey-Nagel silica gel (0.063−0.2 mm) or over Pharmacia Sephadex LH-20. Phosphate buffer (ionic strength 0.1 M) was 0.049 M $KH_2PO_4$, pH adjusted to 7.0 with a 1 M NaOH solution.

**Preparation and Modification of Glassy Carbon Electrodes**. Homemade glassy carbon sticks (typically 0.65 mm diameter) were prepared from glassy carbon rods (Tokai Corp., GC 20S, 3 mm diameter). They were embedded in epoxy resin

* To whom correspondence should be addressed.

10.1021/ma990560m CCC: $18.00 
Published on Web 08/13/1999

(Torr Seal, Varian) and used as disk electrodes. The geometric area of this electrode was determined by comparison of the anodic peak heights obtained by cyclic voltammetry, at a potential scan rate of 0.1 V/s in the presence of ferrocene in acetonitrile, with the thus-prepared electrode and with the 3 mm diameter disk electrode. The electrodes were freshly polished before each derivatization experiment, using successively silicon carbide grinding paper (Struers, grit 500 and 1200) and polishing cloths (Struers) with 6 and 1 $\mu$m diamond powder suspensions. The last polishing step was carried out in the presence of 1 M ammonia. The electrodes were rinsed with dichloromethane under ultrasonic agitation between each polishing step. The derivatized electrodes were dried with a hair-dryer and immersed at ambient temperature in a 15−20 mM solution of NHS−$PEG_{3400}$−Fc in phosphate buffer, DMSO (20% volume) being added in the case of NHS−$PEG_{600}$−Fc. For the attachment of a mixed monolayer of NHS−$PEG_{3400}$−Fc and NHS−$PEG_{3400}$−biotin, a solution containing a total concentration of 20 mM in $PEG_{3400}$ was used, and the mole fraction of $PEG_{3400}$−Fc was varied between 0.25 and 1.0. The PEG modified electrodes were removed after 3−24 h and were rinsed with water and methanol. They were finally submitted to a final ultrasonic rinsing in dimethylformamide for 4 min prior to electrochemical studies. When not in use, the modified electrodes were stored in methanol at ambient temperature in the dark. No decrease of the electrochemically active surface coverage was detected after a 2 day storage.

**Instruments**. All potentials were measured at 20 °C and referred to a KCl saturated calomel electrode (SCE). Spectroscopic and electrochemical instruments were the same as previously reported.[5] The cyclic voltammograms were recorded without ohmic drop compensation. The Digisim 2.1 (DIGI; BioAnalytical Systems Inc.)[6] software package was used for the simulation of the cyclic voltammograms.

**Syntheses**. The synthetic routes to the various PEG derivatives are shown in Scheme 1.

**Preparation of the Activated PEG Esters, OH−$PEG_{3400}$−NHS and $PEG_{600}$−$(NHS)_2$.** To a stirred solution of $PEG_{3400}$ monoacid (540 mg, ~0.16 mmol) in dioxane (3 mL) were added *N*-hydroxysuccinimide, NHS (22 mg, 0.19 mmol), and dicyclohexylcarbodiimide, DCC (39 mg, 0.19 mmol). The resulting mixture was stirred at room temperature for 24 h. The 1,3-dicyclohexylurea (DCU) precipitate was removed by filtration. The filtrate was concentrated under reduced pressure to obtain the activated $PEG_{3400}$ monoester, OH−$PEG_{3400}$−NHS, as a crude material. The residue was further dried under vacuum, yielding a white solid that was used as such in the next step. $^1$H NMR ($CDCl_3$): $\delta$ 3.84 (t, $J \sim 6$ Hz, 2 H, O$CH_2$−$CH_2$CONHS), 3.67 (s, ~300 H, $(OCH_2CH_2)_n$), 2.93 (t, $J \sim 6$ Hz, 2 H, C$H_2$−CONHS), 2.87 (s, 4 H, CONHS). The same procedure was applied to the preparation of $PEG_{600}$−$(NHS)_2$, the bis(succinnimidyl) derivative of the $PEG_{600}$ diacid, except that the amounts of DCC and NHS were doubled. $^1$H NMR ($CDCl_3$): $\delta$ 4.56 (s, 4 H, O$CH_2$CONHS), 3.79−3.67 (m, ~58 H, $(OCH_2CH_2)_n$), 2.87 (s, 8 H, CONHS). TLC ($^i$PrOH/$H_2O$/concentrated ammonia (10:2:1)) gave, for the crude $PEG_{3400}$ monoester and $PEG_{600}$ diester, the expected chromatograms: $R_f = 0.46$ and $R_f = 0.49$, respectively.[7] $^1$H NMR analysis did not exhibit any evidence of unreacted PEG acid in the samples. The dicyclohexyl (DCC + DCU)/PEG mole ratio in the samples was derived from the comparison of the overall integral of the $^1$H NMR methylene signals recorded in the 2.0−1.0 ppm region with that of the polymer backbone ($\delta \sim 3.67$ ppm) and was found typically to be 2.5. For the evaluation of the average molecular weight of each sample, the weight content of residual unreacted NHS was neglected.

**Preparation of OH−$PEG_{3400}$−Fc**. A 280 mg sample of OH−$PEG_{3400}$−NHS (~0.13 mmol of available NHS groups) was dissolved in 1 mL of chloroform and treated with an excess of $\beta$-aminoethylferrocene (40 mg, 0.19 mmol) and triethylamine (27 $\mu$L, 0.19 mmol). After stirring for 16 h, the reaction mixture was evaporated under reduced pressure and chromatographed on silica gel in chloroform−methanol (90:10). The yellow fraction was collected and evaporated. The residue was then purified on Sephadex LH-20 from low molar weight ferrocenes using methanol as an eluent. After solvent removal, the solid residue was stirred in lukewarm 2-propanol (10 mL), filtered, and then washed with 2-propanol (3 × 10 mL) to completely remove remaining dicyclohexyl derivatives and NHS. Drying in vacuo yielded analytically pure OH−$PEG_{3400}$−Fc (270 mg, MW ~ 3700, 56%) as shown chromatographically (TLC, 10% methanol in chloroform, $R_f = 0.45$) and spectroscopically. $^1$H NMR ($CDCl_3$): $\delta$ 6.58 (br. s, 1 H, NHCO), 4.16 (s, 5 H, CpH), 4.11 (app d, 4 H, CpH), 3.67 (s, ~310 H, $(OCH_2CH_2)_n$), 3.42 (t, $J \sim 7$ Hz, 2 H, C$H_2$−NHCO), 2.57 (t, $J \sim 7$ Hz, 2 H, $CH_2$ α to Fc), 2.49 (t, $J \sim 6$ Hz, 2 H, NHCO−C$H_2$).$^{13}$C NMR ($CDCl_3$): $\delta$ 171.26, 85.48, 72.42, 70.18, 68.45, 68.11, 67.33, 67.12, 61.55, 40.38, 36.85, 29.53.

**Scheme 1**

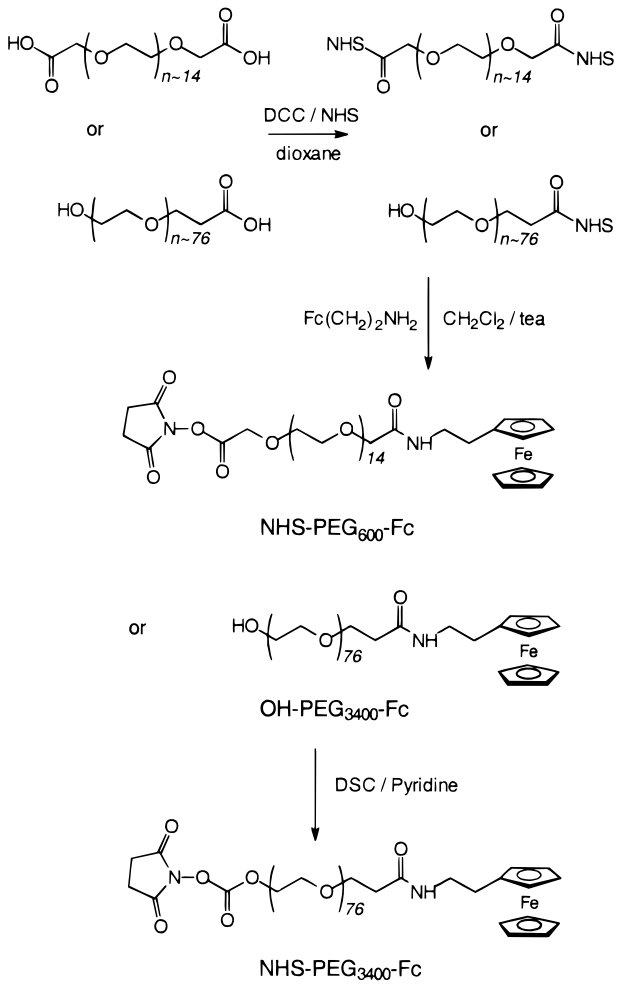


**Preparation of NHS−$PEG_{3400}$−Fc**. Poly(ethylene glycol)-ferrocene, HO−$PEG_{3400}$−Fc (70 mg, ~ 0.019 mmol), was dissolved in dichloromethane (42 $\mu$L), pyridine (9.4 $\mu$L), and acetonitrile (17 $\mu$L). The solution was treated with *N*,*N*-disuccinimidyl carbonate (DSC) (11.6 mg, 0.046 mmol) and stirred for 24 h at room temperature. Cold ethyl ether (4 mL) was added to the solution. The precipitate was collected by filtration and chromatographed on silica gel in chloroform−methanol (90:10). Solvent removal followed by drying in vacuo over $CaCl_2$ afforded NHS−$PEG_{3400}$−Fc as a light yellow solid (55 mg, MW ~ 3800, 78%). $^1$H NMR ($CDCl_3$): $\delta$ 6.62 (br s, 1 H, NHCO), 4.43 (m, 2 H, C$H_2$−$CO_2$NHS), 4.16 (s, 5 H, CpH), 4.11 (app d, 4 H, CpH), 3.79 (m, 2 H, O$CH_2CH_2$−$CO_2$NHS), 3.68 (s, ~310 H, $(OCH_2CH_2)_n$), 3.43 (t, $J \sim 7$ Hz, 2 H, C$H_2$−NHCO), 2.88 (s, 4 H, NHS), 2.58 (t, $J \sim 7$ Hz, 2 H, $CH_2$ α to Fc), 2.50 (t, $J \sim 6$ Hz, 2 H, NHCO−C$H_2$).$^{13}$C NMR ($CDCl_3$): $\delta$ 171.28, 168.42, 136, 85.48, 70.43, 68.46, 68.10, 68.20, 67.33, 67.11, 40.39, 36.85, 29.54, 25.31.

**Preparation of NHS−$PEG_{600}$−Fc**. A 138 mg sample of activated PEG diester $PEG_{600}$−$(NHS)_2$ (~0.29 mmol of avail-

able NHS groups) was dissolved in 1 mL of chloroform and treated with $\beta$-aminoethylferrocene (28.4 mg, 0.19 mmol) and triethylamine (31 $\mu$L, 0.22 mmol). After stirring overnight, condensation reaction was shown to be quantitative by TLC (5% methanol in chloroform). The reaction mixture was evaporated under reduced pressure and chromatographed on silica gel in chloroform/methanol (95:5). The yellow fraction was collected and evaporated to dryness to afford the desired derivative NHS−$PEG_{600}$−Fc as a crude sample. Absence of unconverted PEG ester was checked out by TLC analyses. No effort was made to purify the monosubstituted NHS−$PEG_{600}$−Fc derivative from the bridged bis-ferrocene Fc−$PEG_{600}$−Fc other than filtrating its phosphate solution (Millipore, 0.5 $\mu$m HF) before use for glassy carbon derivatization. Given the proportion of homobifunctional spacer $PEG_{600}$−$(NHS)_2$ allowed to react with the ferrocene reagent, the crude sample was theoretically expected to contain NHS−$PEG_{600}$−Fc and Fc−$PEG_{600}$−Fc in approximately equimolar amounts (ratio 0.66:0.62).[8] This was confirmed by the experimental value derived from the ratio of the integrated $^1$H NMR singlet due to the activated NHS ($\delta$ 2.86 ppm) and the triplet from the methylene group $FcCH_2$ ($\delta$ 2.61 ppm, $J \sim 7$ Hz), the latter signal being common to the two ferrocene−PEG derivatives. Other signals observed in the NMR spectrum of the crude sample were as follows: $\delta$ 7.07 (br s, 1 H, NHCO), 4.22 (s, 0.5 × 2 H, $OCH_2CONHS$), 4.20−4.11 (m, 9 H, CpH), 4.02 (s, 2 H, $OCH_2$−CONH), 3.79−3.68 (~40 H, $(OCH_2CH_2)_n$), 3.43 (m, 2 H, $CH_2$−NHCO).

## Results

The $PEG_{600}$−Fc and $PEG_{3400}$−Fc modified glassy carbon disk electrodes were prepared as described in the Experimental Section and were quite stable. The voltammetric study of the $PEG_{MW}$−Fc modified electrodes was carried out in the presence of a solution of 0.5 M $NBu_4PF_6$ in dichloromethane.

Typical cyclic voltammograms are reproduced in Figure 1 before and after background current correction. At a slow potential scan rate ($v$) of 0.2 V/s remarkably symmetrical anodic and cathodic peaks are recorded. The potentials of the anodic and cathodic peaks differ by less than 10 mV, and for each peak the width at mid-peak height is 95 ± 5 mV as expected theoretically for the behavior of surface adsorbed redox species or for redox species located in a thin layer covering the electrode surface when their flexibility is high compared to the time window of the experiment.[9] Even at low potential scan rates such an almost ideal behavior is not commonly observed[10,11] when redox centers are attached through long arms at an electrode surface.[1,4,12−22] It indicates a homogeneous environment around the redox centers and an absence of interactions between them.[23] The same conclusions are no longer valid when the solvent and supporting electrolyte are water and 1 M $NaClO_4$ instead of $CH_2Cl_2$ and 0.5 M $NBu_4PF_6$. Then the peaks become much broader.

At $v = 0.2$ V/s, the total amount $\Gamma_T$ of attached redox probes $Fc/Fc^+$ can be deduced quantitatively from the area under either the anodic or cathodic peak.[4] Upon increasing the potential scan rate up to at least 200 V/s, both the anodic and cathodic peaks are drawn out as can be seen in Figure 1. At high enough $v$, the anodic ($E_{pa}$) versus cathodic ($E_{pc}$) peak-to-peak separation, $\Delta E_P = E_{pa} - E_{pc}$, may become quite large (see Figure 2). The comparison between the cyclic voltammograms given by a series of modified electrodes shows that, at a given $v$, $\Delta E_P$ does not vary to a large extent (Figure 2). Once they are normalized versus $\Gamma_T$, the peak currents are satisfactorily reproducible as can be seen in Figure 2. The $i_{pa}/\Gamma_T v^{1/2}$ standard deviation for a series of 10

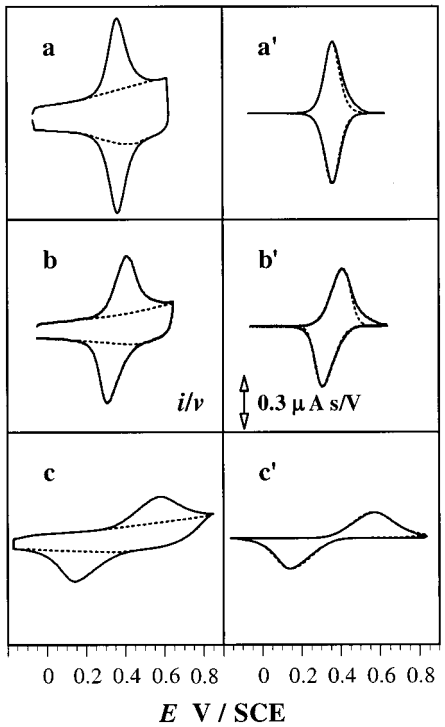


**Figure 1.** Dependence of the cyclic voltammograms on the potential scan rate $v$. $PEG_{3400}$−Fc attached to a glassy carbon electrode. $\Gamma_T = 4.18 \times 10^{-13}$ mol, geometric electrode area $A = 0.0045$ cm$^2$. Currents are normalized vs $v$. $v = 0.2$, 20, and 200 V/s for a,a′, b,b′, and c,c′ respectively. In a, b, and c the dotted lines show the background current recorded before attachment of $PEG_{3400}$−Fc. In a′, b′, and c′ the continuous curves are the background corrected currents; the dotted curves, not apparent when superposed on the continuous ones, are the simulated cyclic voltammograms obtained as described in the text for $k_s/D_{Fc}^{1/2} = 15.4$ s$^{-1/2}$, $D_{Fc}^{1/2}/e = 29.15$ s$^{-1/2}$, $D_{Fc^+}/D_{Fc} = 2.00$, $C_{dl} = 0.8 \times 10^{-7}$ farad, and $R_u = 1800$ Ω.

$PEG_{3400}$−Fc derivatized electrodes amounts to 6%, $i_{pa}$ being the anodic peak current.

Similar results are obtained when the $PEG_{3400}$−Fc electrode coverage $\Gamma_T$ is decreased from $\Gamma_T = 4.18 \times 10^{-13}$ to $2.19 \times 10^{-13}$ mol by simultaneous coattachment of $PEG_{3400}$−Fc and $PEG_{3400}$−biotin. The reason for the choice of biotinylated $PEG_{3400}$ as a surface diluting agent is twofold. First, biotin is not electroactive in the explored potential range; second, the NHS−$PEG_{3400}$−biotin reagent is commercially available and has been already used for the covalent attachment of long arm biotin to glassy carbon surfaces.[3] The $PEG_{3400}$−Fc electrode coverage $\Gamma_T$ was also decreased to $3.23 \times 10^{-13}$ mol, in the absence of diluting PEG reagent, when the time allowed for the reaction between the ammonia polished glassy carbon surface and NHS−$PEG_{3400}$−Fc was shortened.[2] We also found that a change in the supporting electrolyte concentration, from 0.5 to 0.3 M $NBu_4PF_6$, does not affect appreciably the observed behavior once the ensuing change in solution resistance is taken into account.

Very similar results were also obtained with $PEG_{600}$−Fc modified electrodes as shown in Figure 2. We did not proceed to surface dilution by simultaneous coattachment of an electrochemically inactive PEG derivative. When the $PEG_{600}$−Fc coverage $\Gamma_T$ was varied ($3.12 \times 10^{-13} \leq \Gamma_T \leq 4.08 \times 10^{-13}$ mol) simply by adjustment of the time during which the ammonia polished glassy carbon surface and NHS−$PEG_{600}$−Fc were allowed to react, the essential features of the cyclic voltammo-

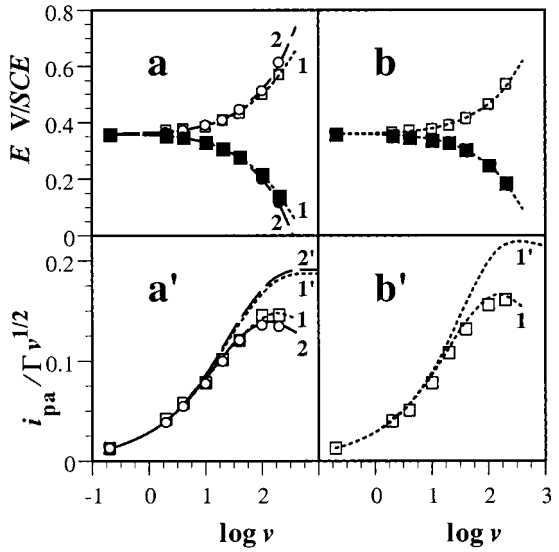


**Figure 2.** Potential scan rate $v$ dependence of the peak potentials $E_{pa}$ and $E_{pc}$ and of the anodic peak current $i_{pa}$ normalized versus $\Gamma_T$ and $v^{1/2}$. Units for $i_{pa}/\Gamma_T v^{1/2}$: $\mu$A s$^{1/2}$/mol V$^{1/2}$; units for $v$: V/s. Geometric electrode area $A = 0.0045$ cm$^2$. a and a′: PEG$_{3400}$−Fc modified electrode. □, ○ for $\Gamma_T = 4.18$ and 2.19 (+ PEG$_{3400}$−biotin) × $10^{-13}$ mol, respectively. Dotted curves 1 and 1′ give the simulated values obtained as described in the text for the first $\Gamma_T$, $k_s/D_{Fc}^{1/2} = 15.4$ s$^{-1/2}$, $D_{Fc}^{1/2}/e = 29.15$ s$^{-1/2}$, $D_{Fc^+}/D_{Fc} = 2.00$, $C_{dl} = 0.8 \times 10^{-7}$ farad, and $R_u = 1800$ (1) or 0 (1′) Ω. Dashed curves 2 and 2′ give the simulated values for the second $\Gamma_T$ (same units), $k_s/D_{Fc}^{1/2} = 18.6$, $D_{Fc}^{1/2}/e = 29.6$, $D_{Fc^+}/D_{Fc} = 1.86$, $C_{dl} = 10^{-7}$, and $R_u = 3200$ (2) or 0 (2′). b and b′: PEG$_{600}$−Fc modified electrode, $\Gamma_T = 3.56 \times 10^{-13}$ mol. Dotted curves 1 and 1′ give the simulated values (same units) for $k_s/D_{Fc}^{1/2} = 74.5$, $D_{Fc}^{1/2}/e = 28.5$, $D_{Fc^+}/D_{Fc} = 2.00$, $C_{dl} = 1.3 \times 10^{-7}$, and $R_u = 1600$ (1) or 0 (1′).

grams, particularly the potential scan rate dependence, remained unchanged.

The geometric area $A$ of the glassy carbon electrode we used was 0.0045 cm$^2$. Therefore, the surface concentrations of attached ferrocenes per unit of geometric area ($\Gamma_T/A$) lay between 7.2 and 9.3 × $10^{-11}$ mol/cm$^2$ range. Each ferrocene pertains to a PEG chain. Taking into account a roughness factor of the glassy carbon surface of ca. 3,[24] the average of effective electrode area allowed for the attachment of one PEG$_{MW}$−Fc chain lay in the 5.4−6.9 nm$^2$ range. That gives for the average distance $d$ between terminally attached PEG chains $2.3 \leq d \leq 2.6$ nm.

## Discussion

The most striking feature of the experimental results is that, whatever the potential scan rate, the cyclic voltammograms obtained with electrodes bearing either terminally attached PEG$_{3400}$−Fc or PEG$_{600}$−Fc are very similar. The time responses are very close in both configurations.

To characterize quantitatively the flexibility of the ferrocene redox centers linked to one end of the PEG long arms whose other end is covalently attached to the glassy carbon surface, models to figure out how the electroactive Fc groups can reach the electrode surface are required. We considered two simple models. The first consists of assuming that the ferrocene redox centers are adsorbed at the electrode surface. Such a configuration implies that the random coil[25] of the PEG chain lay mostly flat on the electrode surface as sketched in Figure 3a. In the second model, the PEG coil is mostly perpendicular to the electrode surface, and the electron

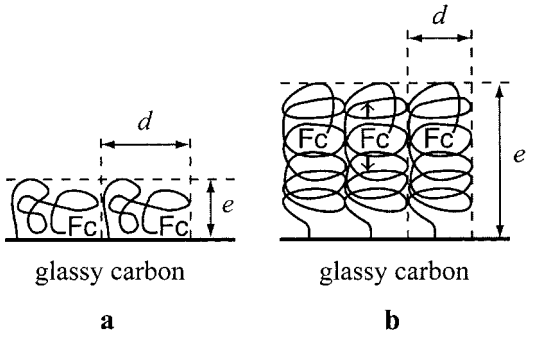


**Figure 3.** The two models of configurations of the attached PEG chains: (a) adsorption like; (b) the PEG coil is mostly perpendicular to the electrode surface.

transfer takes place only when the Fc end of the PEG chain reaches the electrode surface through motion, as sketched in Figure 3b.

**Adsorption-like Behavior**. Obviously, identical time responses would be obtained if the Fc heads of the terminally attached PEG$_{600}$−Fc and PEG$_{3400}$−Fc chains were, in both cases, adsorbed at the glassy carbon surface. Thus, the adsorption model could simply explain the near identity of the measured time responses.

When there is no significant interaction between the adsorbed species, the electron transfer may obey the Nernst law at sufficiently low potential scan rate $v$. Then the main features of the cyclic voltammogram are as follows: the anodic and cathodic peak potentials are identical ($\Delta E_P = 0$) and equal to the standard potential ($E°_{Fc/Fc^+}$) of the ferrocene/ferricenium (Fc/Fc$^+$) redox couple, and the peak width at mid-peak height is 90 mV.[9] As already mentioned, and shown in Figure 1, we observed such a behavior at $v = 0.2$ V/s. In these circumstances, the value of the anodic or cathodic nernstian peak current, normalized versus $v$ and $\Gamma_T$, is $(i_{pa}/\Gamma_T v)_{nernst} = (i_{pc}/\Gamma_T v)_{nernst} = 0.25(F^2/RT)$.[4]

According to the adsorption model, the observed increase in the peak-to-peak separation $\Delta E_P$ with increasing $v$ would then result from the slowness of the electron transfer and additionally from the ohmic drop caused by the uncompensated resistance ($R_u$) of the electrochemical cell. Concomitantly, due to the slowness of the electron transfer, the $i_{pa}/\Gamma_T v$ ratio should decrease with increasing $v$ down to a lower limit that is reached when the electron transfer is practically irreversible, i.e., when $\Delta E_P \geq 200$ mV. The lower limit is $(i_{pa}/\Gamma_T v)_{irrev} = (F^2/RT)(1 - \alpha)\exp(-1)$, α being the transfer coefficient, and the lower limit of $(i_{pc}/\Gamma_T v)_{irrev}$ is $(F^2/RT)\alpha \exp(-1)$.[23] The peak shapes also depend on α. When $\alpha = 0.5$, the widths of the anodic and cathodic peaks are identical. When $\alpha > 0.5$, the anodic peak becomes broader while the cathodic one is comparatively sharper and higher.[23,26] The shapes of the cyclic voltammograms reproduced in Figure 1 show that the condition $\alpha > 0.5$ should hold if the adsorption were relevant. Not taking into account the effect of ohmic drop (i.e., assuming that $R_u = 0$), the ratio $(i_{pa}/\Gamma_T v)_{v=200}/(i_{pc}/\Gamma_T v)_{v=0.2}$ should not be less than 0.59 for α as high as 0.6. The effect of the ohmic drop on the experimental data can be corrected as explained later on, and the correction yields the computed curves reproduced in Figure 2a′,b′ for $R_u = 0$. The value of the ratio $(i_{pa}/\Gamma_T v)_{v=200}/(i_{pc}/\Gamma_T v)_{v=0.2}$ which can be derived from these curves is slightly smaller than 0.5 and thus significantly smaller than 0.59. The adsorption-like model must be discarded since it cannot justify the observed dependence of the peak currents on the potential scan rate $v$ at high $v$.

The rejection of the adsorption-like model is also in agreement with what is known concerning the structure of the $PEG_{3400}$ coil. The degree of polymerization ($N$) of $PEG_{3400}$ being 77, the random coil model gives a Flory radius (end-to-end distance) of 4.65 nm and a radius of gyration of 1.9 nm for the polymer at equilibrium in a $\Theta$ solvent[25,27] or 5.15 and 2.1 nm respectively for the Flory and gyration radii in a good solvent.[25,28] The average distance between terminally attached PEG chains $d$ that we estimated in the preceding section ($2.3 \leq d \leq 2.6$ nm) is smaller than the Flory radius. Thus, the PEG coil cannot lay flat on the electrode surface, i.e., with its longest axis parallel to the electrode surface. Twice the radius of gyration of $PEG_{3400}$−Fc at equilibrium is also greater than $d$. Therefore, the $PEG_{3400}$ coil is constrained to some stretching toward the solution or squeezed like in a tube.[25,29−32] A similar situation has been reported recently for thiolated $PEG_{5000}$ polymers bound to nanometer gold clusters.[33]

A Flory radius of 1.82 nm ($\Theta$ solvent) or 1.95 nm (good solvent) can be similarly calculated for the $PEG_{600}$ random coil. In that case the PEG coil could theoretically lay flat on the electrode surface. However, as demonstrated by the potential scan rate dependence of the voltammetric signals, the adsorption-like model is still inadequate to justify the observed behavior of terminally attached $PEG_{600}$−Fc.

**Quantitative Analysis in Terms of Finite Linear Diffusion**. Now we consider that the Fc and $Fc^+$ redox centers diffuse to and from the electrode surface, with apparent diffusion coefficients $D_{Fc}$ and $D_{Fc^+}$, within a layer of thickness $e$ equal to the average length of the attached $PEG_{MW}$−Fc chains. The initial distribution of the Fc heads within the thin layer is taken as homogeneous. The cyclic voltammograms corresponding to this model can be simulated rather easily at the thermostated temperature of 20 °C. Besides $D_{Fc}$, $D_{Fc^+}$, $\Gamma_T$, and $e$, the parameters required for the simulation are the standard rate constant of the heterogeneous electron transfer ($k_S$ in cm/s), its transfer coefficient, taken as $\alpha = 0.5$, the double-layer capacitance $C_{dl}$, and the uncompensated resistance $R_u$. To obtain the best fit between the experimental cyclic voltammograms and the simulated ones, we proceeded as follows. First of all, the double-layer capacitance $C_{dl}$ was adjusted so as to reproduce the background current at the beginning of the voltammogram. At any $v$, $R_u$, and $C_{dl}$, both the peak potentials and the peak currents depend on $k_S/D_{Fc}^{1/2}$ for the anodic peak (or $k_S/D_{Fc^+}^{1/2}$ for the cathodic peak) and $D_{Fc}^{1/2}/e$ (or $D_{Fc^+}^{1/2}/e$ for the cathodic peak).[34] The thickness of the diffusion layer decreases with increasing $v$. Therefore, the contribution of diffusion to the kinetic control of the signal response increases. At each $v$ the parameters $R_u$, $k_S/D_{Fc}^{1/2}$, $k_S/D_{Fc^+}^{1/2}$, $D_{Fc}^{1/2}/e$, and $D_{Fc^+}^{1/2}/e$ were finely tuned to fit the background corrected experimental curves with the simulated ones, after subtraction of the capacitive current. Typical examples of the fits given by the same set of parameters over the whole range of explored $v$ (0.2−200 V/s) are reproduced in Figure 1. For the peak potentials and the anodic peak current the resulting fits are shown in Figure 2.

The fact that $D_{Fc^+} > D_{Fc}$ could be inferred, without any computation, from the comparison of the shapes of the voltammetric peaks when $v$ is high enough to bring about a departure from the symmetry observed at low $v$. Then diffusion becomes involved in the kinetic control of the process. The cathodic peak being sharper and higher than the anodic one (see Figure 1) implies necessarily that $D_{Fc^+} > D_{Fc}$. The best fits give a $D_{Fc^+}/D_{Fc}$ ratio of $1.9 \pm 0.1$. The cause of the observed discrepancy between $D_{Fc}$ and $D_{Fc^+}$ cannot be ascribed to ion pairing of $Fc^+$ with the anion of the supporting electrolyte or to the slowness of diffusion of the latter which must move to maintain local electric neutrality, since the $D_{Fc^+}/D_{Fc}$ ratio is not affected by a change in supporting electrolyte concentration. As far as one is interested only in the value of anodic peak current, the computation shows that taking $D_{Fc^+} = D_{Fc}$ does not cause significant change.

The $k_S/D_{Fc}^{1/2}$ and $D_{Fc}^{1/2}/e$ parameters determined for each modified electrode were used to compute the $i_{pa}/\Gamma_T v^{1/2}$ ratio at $R_u = 0$. That gives the $v$ dependence of $i_{pa}/\Gamma_T v^{1/2}$, free of uncompensated ohmic drop interference (see examples in Figure 2a′,b′). The new $i_{pa}/\Gamma_T v^{1/2}$ vs log $v$ plots thus obtained always exhibit a plateaulike shape at $v \geq 200$ V/s. Such a plateau is reached when the thickness of the diffusion layer becomes smaller than the average length $e$ of the attached $PEG_{MW}$−Fc chains.[35] Simultaneously, due to the small value of $k_S/(D_{Fc}v)^{1/2}$, the heterogeneous electron transfer proceeds almost irreversibly. Then the corresponding anodic peak current $i_{pa,v>200}$ (in $\mu$A) is $0.299\alpha^{1/2}AC°_{Fc}(D_{Fc}v)^{1/2}$, with $C°_{Fc}$ the volume concentration of redox centers (in mol/cm$^3$).[35] As $\Gamma_T = eAC°_{Fc}$, the $i_{pa,v>200}/\Gamma_T v^{1/2}$ ratio depends only on $D_{Fc}^{1/2}/e$, i.e., on the time response $e^2/D_{Fc}$. We found $e^2/D_{Fc} = (1.13 \pm 0.15) \times 10^{-3}$ s and $e^2/D_{Fc} = (1.30 \pm 0.18) \times 10^{-3}$ s for the attached $PEG_{3400}$−Fc and $PEG_{600}$−Fc, respectively.

As already underlined, the most striking result is the near identity of the time responses ($e^2/D_{Fc}$) of the $PEG_{3400}$−Fc and $PEG_{600}$−Fc derivatized electrodes. The $PEG_{3400}$−Fc layer thickness ($e_{3400}$) is inherently larger than the $PEG_{600}$−Fc layer thickness ($e_{600}$). Therefore, the apparent diffusion coefficient of the ferrocene redox probe of the attached $PEG_{3400}$−Fc ($D_{Fc,3400}$) is necessarily greater than that of the attached $PEG_{600}$−Fc ($D_{Fc,600}$). The surface coverage $\Gamma_T$ and the electrode area being similar in both cases, the volume concentration $C°_{Fc}$ of the redox centers ($Fc + Fc^+$) is inversely proportional to the PEG layer thickness; thus, $C°_{Fc,600} > C°_{Fc,3400}$.

The rate of electron hopping, between redox centers able to reach the electrode surface and redox centers located farther, increases with increasing $C°_{Fc}$. Presently, kinetic control of the observed current by electron hopping can be excluded since the experimental data indicate the opposite trend: $D_{Fc,3400} > D_{Fc,600}$ when $C°_{Fc,3400} < C°_{Fc,600}$.

The PEG layer thickness $e_{600}$ and $e_{3400}$ can be "scaled" as follows.[25] The Flory radius of $PEG_{600}$−Fc ($R_{F,600} \approx 1.9$ nm) is smaller than the average distance $d$ separating terminally attached PEG chains ($d \approx 2.5$ nm). Then $e_{600} \approx R_{F,600}$.[30] In the case of $PEG_{3400}$−Fc, $d$ is smaller than either the Flory radius ($R_{F,3400} \approx 5$ nm) or twice the radius of gyration ($2R_{g,3400} \approx 4$ nm) of the macromolecule. As a result, the attached $PEG_{3400}$−Fc coils are overlapping and the chains are stretched. In this regime, $e_{3400}$ becomes proportional to the average number ($N$) of monomers per chain.[29,30] For $PEG_{3400}$ $N = 77$. According to a more detailed approach $e_{3400} \approx pNa\sigma^{1/3}$, $a$ being the monomer size, $\sigma$ ($=a^2/d^2$) the graft density, and $p$ a proportionality coefficient ($p < 1$).[31,32] The lowest possible value of $a$ (0.278 nm) is given by the X-ray structural analysis of PEG crystals;[32] its highest possible value ($a \approx 0.376$ nm) can be derived from the Flory

radius determined in a good solvent into which the PEG chain is swollen ($R_F \approx aN^{0.6}$).[25,27,28] Taking $a \approx 0.3$ nm would give $e_{3400} \approx 5.6p$ nm with a proportionality coefficient $p$ which can be as small as 0.5.[31,32] Eventually, we can reasonably estimate that $e_{3400}/e_{600} \approx 1.5-3$ and $D_{Fc,3400}/D_{Fc,600} \approx 3-10$.

**Effect of the PEG Chain Elasticity**. At this point it must be recalled that $D_{Fc,3400}$ and $D_{Fc,600}$ are only apparent diffusion coefficients. At any time $t$, the dynamics of the Fc heads perpendicular to the electrode surface result from the effect of several forces. Assuming that the elasticity of the PEG chain can be mimicked by an harmonic oscillator, the springlike force $F_{spr}$ that tends to bring back the ferrocene head to its resting position is $F_{spr} = -k_{spr}x$, $k_{spr}$ being a spring constant and $x$ measuring the spring elongation away from the resting position of the ferrocene head. The oxidation of Fc at the electrode surface gives rise to a concentration gradient and an osmotic force $F_{os} = -(k_BT/C_x)(\partial C/\partial x)$, with $k_B$ the Boltzmann constant and $C_x$ the ferrocene volume concentration at the spatial position defined by $x$. When the Fc head moves, a drag force $F_{dr} = -k_{dr}V$ must be overcome, with $k_{dr}$ the corresponding drag coefficient and $V$ the velocity of the Fc head. At the time scale of molecular motion, the ferrocene head reaches a stationary velocity $V_l$ and

$$\frac{k_BT}{C}\frac{\partial C}{\partial x} + k_{spr}x + k_{dr}V_l = 0 \qquad (1)$$

The flux $J_{x,t}$ of Fc at time $t$ through the plane of altitude $x$ is given by $J_{x,t} = CV_l$, and the above equation leads to the following expression for the flux under conditions of elastic bounded diffusion

$$J_{x,t} = -\frac{k_BT}{k_{dr}}\frac{\partial C}{\partial x} - \frac{k_{spr}}{k_{dr}}Cx = -D\left(\frac{\partial C}{\partial x} + \frac{k_{spr}}{RT}Cx\right) \qquad (2)$$

the diffusion coefficient $D$ being related to the drag coefficient by the Einstein relation ($D = k_BT/k_{dr}$) and the spring constant $k_{spr}$ being then defined as a molar quantity.

At equilibrium

$$J_{x,t} = 0 \quad \text{and} \quad C_x = C_{x=0}\exp\left(-\frac{k_{spr}}{2RT}x^2\right) \qquad (3)$$

In cyclic voltammetry the anodic peak current is proportional to $J_{xel}$ given by eq 2 for $x = x_{el}$, which locates the electrode surface relative to the resting position of the Fc head.

The dynamics of the $Fc^+$ heads can be described similarly. However, a supplementary term corresponding to an electromotive force must be introduced in eq 1. This electromotive force results from the effect of the electric field existing within the double layer created at the electrified interface. The electrode is positively charged, and the $Fc^+$ head bearing a positive charge is repelled away from the electrode surface. That is probably why the apparent diffusion coefficient $D_{Fc^+}$ is greater than $D_{Fc}$.

The above-mentioned equations point to the several key features. First of all, even at equilibrium, i.e., in the absence of faradaic current, the distribution of the Fc heads of the PEG chains is not uniform; it is given by eq 3. Parabolic distributions of the free end of polymer brushes were previously described.[36,37] Second, eq 2 shows that the type of apparent diffusion coefficient we estimated reflects actually a combination of a purely diffusive contribution and an elastic penalty. Both contributions depend on $k_{dr}$, which itself depends on the brush viscosity.[37,38]

On one hand, it seems reasonable to consider that $D$ is greater in the $PEG_{600}$−Fc than in the $PEG_{3400}$−Fc brush, the latter being more compact. On the other hand, the elastic penalty depends also on the spring constant $k_{spr}$. The identity of the time responses of the $PEG_{600}$−Fc and $PEG_{3400}$−Fc brush electrodes suggests that the spring constant is also markedly greater in the former type of derivatized electrode in which the PEG chains could be more elastic since they are not squeezed.

## Conclusion

The NHS−$PEG_{600}$−Fc and NHS−$PEG_{3400}$−Fc chains of markedly different lengths were synthesized and attached, through their NHS activated ends, to the surface of glassy carbon electrodes. The presence of the Fc redox head enabled us to use cyclic voltammetry for a quantitative characterization of the flexibility of terminally attached $PEG_{MW}$−Fc chains. Given the coverage of the electrode surface, the $PEG_{3400}$−Fc chains were constrained to stretch whereas the $PEG_{600}$−Fc chains were not. At sufficiently high potential scan rate the peak height of the current response is controlled by the flexibility of the attached PEG chain. In such circumstances we found almost identical time responses for both types of terminally attached $PEG_{MW}$−Fc chains, an unexpected result which raises interesting questions and stresses the need of further experimental investigation and more elaborate models allowing a quantitative handling of the distribution and diffusion of the loose ends and of the elasticity of the chains.

**Acknowledgment.** The homemade glassy carbon electrodes of small diameter were kindly prepared by Dr. C. P. Andrieux.

## References and Notes

(1) Murray, R. W. Chemically Modified Electrodes. In *Electroanalytical Chemistry*; Bard, A. J., Ed.; Marcel Dekker: New York, 1984; Vol. 13, pp 191−368.
(2) Anne, A.; Blanc, B.; Moiroux, J.; Savéant, J.-M. *Langmuir* **1998**, *14*, 2368.
(3) Anicet, N.; Anne, A.; Moiroux, J.; Savéant, J.-M. *J. Am. Chem. Soc.* **1998**, *120*, 7115.
(4) Finklea, H. O. Electrochemistry of Organized Monolayers of Thiols and Related Molecules on Electrodes. In *Electroanalytical Chemistry*; Bard, A. J., Rubinstein, I., Eds.; Marcel Dekker: New York, 1996; Vol. 19, pp 191−368.
(5) Anne, A.; Moiroux, J.; Savéant, J.-M. *J. Am. Chem. Soc.* **1993**, *115*, 10224−10230.
(6) Rudolph, M.; Reddy, D. P.; Feldberg, S. W. *Anal. Chem.* **1994**, *66*, 589A.
(7) Zalipsky, Z. *Bioconjugate Chem.* **1993**, *4*, 296−299.
(8) Simons, D. M. *Bioconjugate Chem.* **1999**, *10*, 3−8.
(9) Laviron, E. Voltammetric Methods for the Study of Adsorbed Species. In *Electroanalytical Chemistry*; Bard, A. J., Ed.; Marcel Dekker: New York, 1982; Vol. 12, pp 53−157.
(10) Ravenscroft, M. S.; Finklea, H. O. *J. Phys. Chem.* **1994**, *98*, 3843.
(11) Hirst, J.; Armstrong, F. A. *Anal. Chem.* **1998**, *70*, 5062.
(12) Itaya, K.; Bard, A. J. *Anal. Chem.* **1978**, *50*, 1487.
(13) Lenhard, J. R.; Murray, R. W. *J. Am. Chem. Soc.* **1978**, *100*, 7870.
(14) Wrighton, M. S.; Austin, R. G.; Bocarsly, A. B.; Bolts, J. M.; Haas, O.; Legg, K. D.; Nadjo, L.; Palazzotto, M. *J. Electroanal. Chem.* **1978**, *97*, 429.
(15) Smith, D. F.; Willman, K.; Kuo, K.; Murray, R. W. *J. Electroanal. Chem.* **1979**, *95*, 217.

(16) Fischer, A. B.; Wrighton, M. S.; Umana, M.; Murray, R. W. *J. Am. Chem. Soc.* **1979**, *101*, 3442.
(17) Zou, C.; Wrighton, M. S. *J. Am. Chem. Soc.* **1990**, *112*, 7578.
(18) Finklea, H. O.; Hanshew, D. D. *J. Am. Chem. Soc.* **1992**, *114*, 3173.
(19) Rowe, G. K.; Creager, S. E. *Langmuir* **1991**, *7*, 2307.
(20) Rowe, G. K.; Creager, S. E. *J. Phys. Chem.* **1994**, *98*, 5500.
(21) Creager, S. E.; Rowe, G. K. *J. Electroanal. Chem.* **1997**, *420*, 291.
(22) Sabapathy, R. C.; Bhattacharyya, S.; Leavy, M. C.; Cleland, W. E.; Hussey, C. L. *Langmuir* **1998**, *14*, 124.
(23) Laviron, E. *J. Electroanal. Chem.* **1979**, *101*, 19.
(24) Andrieux, C. P.; Gonzalez, F.; Saveant, J. M. *J. Am. Chem. Soc.* **1997**, *119*, 4292.
(25) de Gennes, P. G. *Scaling Concepts in Polymer Physics*; Cornell University Press: Ithaca, NY, 1991; pp 29−53, 165−204.
(26) Laviron, E. *J. Electroanal. Chem.* **1979**, *100*, 263.
(27) Klein, J.; Luckham, P. *Macromolecules* **1984**, *17*, 1041.
(28) Vincent, B.; Luckham, P.; Waite, F. A. *J. Colloid Interface Sci.* **1980**, *73*, 508.
(29) Alexander, S. *J. Phys. (Paris)* **1977**, *38*, 983.
(30) de Gennes, P. G. *Macromolecules* **1980**, *17*, 1069.
(31) Patel, S.; Tirrell, M.; Hadziioannou, G. *Colloids Surf.* **1988**, *31*, 157.
(32) Jeon, S. I.; Lee, J. H.; Andrade, J. D.; de Gennes, P. G. *J. Colloid Interface Sci.* **1991**, *142*, 149.
(33) Wuelfing, W. P.; Gross, S. M.; Miles, D. T.; Murray, R. W. *J. Am. Chem. Soc.* **1998**, *120*, 12696.
(34) Andrieux, C. P.; Savéant, J. M. *J. Electroanal. Chem.* **1980**, *111*, 377.
(35) Nadjo, L.; Savéant, J. M. *J. Electroanal. Chem.* **1973**, *48*, 113.
(36) Pincus, P. *Macromolecules* **1991**, *24*, 2912.
(37) Halperin, A. *Langmuir* **1999**, *15*, 2525.
(38) Halperin, A.; Alexander, S. *Europhys. Lett.* **1986**, *6*, 439.

MA990560M